


RESEARCH

Open Access



Nanofibrous polypeptide hydrogels with collagen-like structure as biomimetic extracellular matrix

Chengkun Zhao^{1,2}, Xing Li^{1,2}, Shaoquan Bian³, Weinan Zeng^{4*}, Alfredo Ronca⁵, Ugo D'Amora⁵, Maria Grazia Raucci⁵, Jie Liang^{1,2}, Yong Sun^{1,2} , Qing Jiang^{1,2*}, Yujiang Fan^{1,2}, Luigi Ambrosio⁵ and Xingdong Zhang^{1,2}

Abstract

Supramolecular peptides exhibit obvious similarities with collagen fibers in terms of self-assembly characteristics, nanofibrous structure, and responsiveness to external stimuli. Here, a series of supramolecular peptides were developed by altering the amino acid sequence, enabling the self-assembly of three types of 4-biphenylacetic acid (BPAA)-tripeptides into fibrous hydrogel through hydrogen bonding and π - π stacking under the influence of ion induction. Transmission electron and scanning electron microscopies revealed that the diameter of the fiber within nanofibrous hydrogels was ~ 10 and ~ 40 nm, respectively, which was similar with the self-assembled collagen fibers. For this reason, these hydrogels could be considered as a biomimetic extracellular substitute. Meanwhile, the gelation concentration induced by ions was even lower than 0.66 wt%, with an elastic modulus of ~ 0.27 kPa, corresponding to a water content of 99.34 wt%. In addition, the three supramolecular hydrogels were found to be good substrates for L929 cell adhesion and MC-3T3 cell proliferation. The overall results implied that BPAA-based hydrogels have a lucrative application potential as cell carriers.

Keywords Collagen-like, Supramolecular peptides, Nanofibrous hydrogel, Ion-induction, Biomimetic extracellular matrix

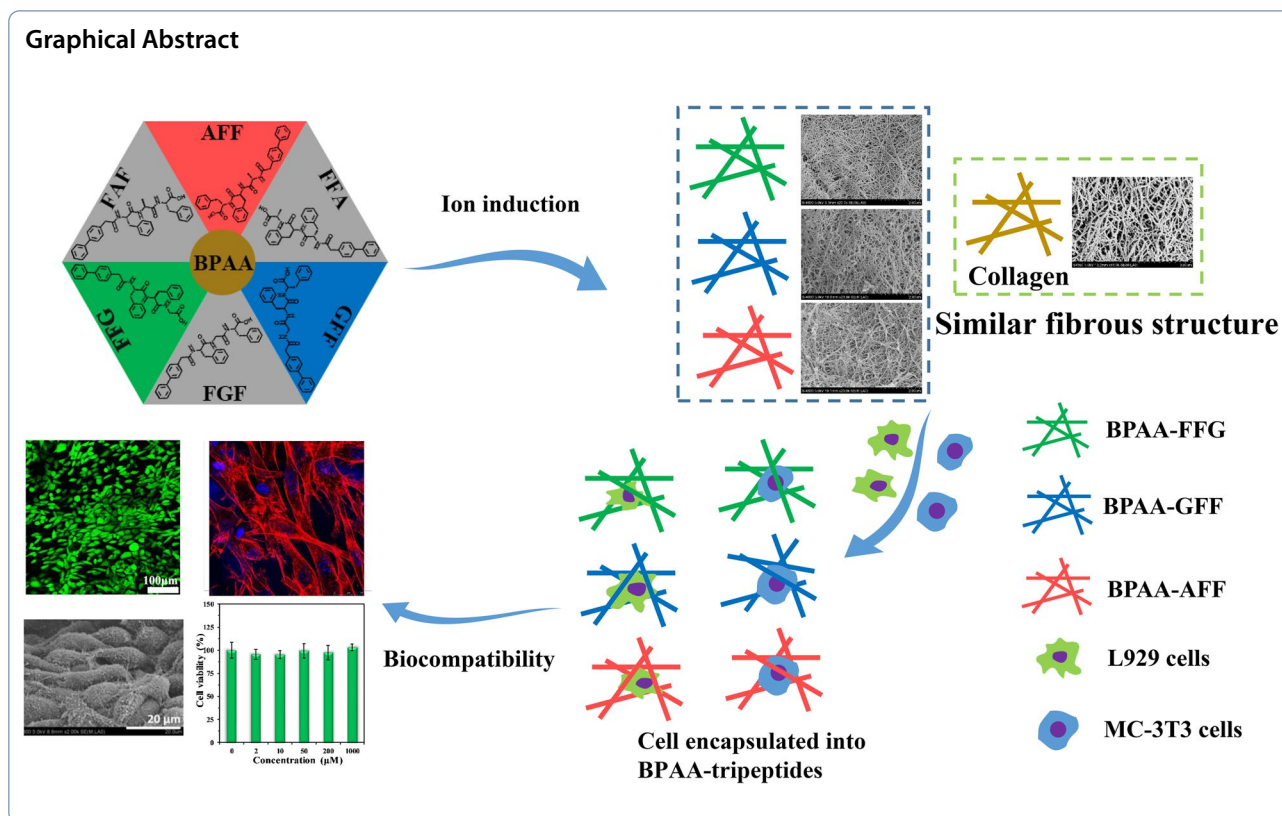
*Correspondence:

Weinan Zeng
weinanzeng@163.com
Qing Jiang
jiangq@scu.edu.cn

Full list of author information is available at the end of the article



© The Author(s) 2023. **Open Access** This article is licensed under a Creative Commons Attribution 4.0 International License, which permits use, sharing, adaptation, distribution and reproduction in any medium or format, as long as you give appropriate credit to the original author(s) and the source, provide a link to the Creative Commons licence, and indicate if changes were made. The images or other third party material in this article are included in the article's Creative Commons licence, unless indicated otherwise in a credit line to the material. If material is not included in the article's Creative Commons licence and your intended use is not permitted by statutory regulation or exceeds the permitted use, you will need to obtain permission directly from the copyright holder. To view a copy of this licence, visit <http://creativecommons.org/licenses/by/4.0/>.



1 Introduction

Collagen is abundant in the connective tissues of human body, especially the skin, joints, and bones [1]. As an extracellular matrix (ECM), collagen has been widely used in cell culture, tissue engineering, and wound healing [2, 3]. Nonetheless, some limitations, including intrinsic immunogenicity, batch-to-batch instability, and a high cost of extraction hindered its development [4, 5]. Therefore, designing an alternative collagen-like gel material with low-cost and biomimetic properties is worth studying and researching [6–8].

In recent years, supramolecular hydrogels were extensively studied and applied in biomedical field. As promising soft materials, with a wide range of applications, supramolecular hydrogels are typically fabricated via directional, tunable, and reversible non-covalent interactions, such as electrostatic effects, Van der Waals' forces, hydrogen bonding, π - π stacking, and metal–ligand complexation between gelators [8, 9]. In addition, small gelators can self-assemble into hydrogels with nanostructured morphology (usually nanofibers, similar to collagen fibers). Recently, supramolecular hydrogels based on fundamental biological molecules, such as amino acids, saccharides, and nucleobases, have been regarded as desirable biomaterials, due to their great biocompatibility and biological properties

[10]. Among them, the most widely applicable motifs for preparing gelators include short peptides.

Numerous remarkable low-molecular-weight gelators (LMWGs) have been developed by combining hydrophobic functional moieties [11]. For instance, the Fluorenylmethoxycarbonyl (Fmoc)-protect group has been used to promote the self-assembly of various short-peptide and amino acid-based derivatives, demonstrating the significance of specific aromatic stacking interactions [12]. Accordingly, these functionalized short peptide gelators have attracted significant interest due to their low cost, easy synthesizability, and responsiveness to external stimuli [13, 14]. Additionally, the ECM-like nanostructures of short peptide hydrogels endow ECM functions, such as the maintenance of cells phenotype and cellular behavior in terms of growth, proliferation and differentiation. Therefore, functionalized short peptide supramolecular hydrogels have demonstrated promising application potential in tissue engineering [15], drug delivery [16], cancer inhibition [17], and cellular imaging [18]. In this regard, Stupp et al. made use of two distinct cell signals to alter the amino sequence for the synthesis of a series of peptide amphiphiles (PAs) with different physiochemical properties, thereby demonstrating that PAs, with greater motion, could physically and computationally lead to greater functional recovery from spinal cord injury in a

murine model [19]. Additionally, Yang et al. synthesized several protein derivatives to selectively degrade the membrane proteins of programmed cell death-ligand 1 in 4T1 cells [20]. Moreover, Xu et al. reported a novel probe including short peptides for imaging the membrane dynamics of living cells, with high spatial and temporal resolution, over extended time scales and areas [21].

Several synthetic aromatic moieties, such as naphthalene, azobenzene, pyrene, and other derivatives, have been employed at the *N*-terminus of dipeptides, to produce remarkable LMWGs (commonly referred to as aromatic short-peptide gelators) [22]. This *N*-terminal aromatic moiety has played a crucial role in the design of aromatic short peptide gelators, by providing strong π - π stacking between aromatic molecules [23]. However, it was hardly reported the choice of biphenyl molecules, as *N*-terminal aromatic moiety, due to a less effective π - π stacking formed by adjacent phenyl groups [24]. Therefore, to expand the scope of *N*-terminal moiety, a 4-biphenylacetic acid (BPAA), one of the intermediates widely used in the synthesis of anti-inflammatory drugs, was selected. Besides, the amino acid composition is crucial for hydrogel fabrication. Because of the ability to self-assemble into nanotube structure, "FF" peptide sequence has been commonly conjugated with *N*-terminal moiety to form hydrogels. Furthermore, "FF-containing" peptides could be activated by external stimuli, such as pH, temperature and ions [25–28].

Therefore, in the current study, FF sequence and BPAA were chosen as amino sequence brick and *N*-terminal moiety. By introducing two common amino acids in the human body, alanine and glycine, six types of BPAA-tripeptides with different amino acid sequences were synthesized. Then, the varying gelation properties and supramolecular architectures of hydrogels induced by ion induction of the different gelators were deeply investigated, the aim being to demonstrate the great potential of these peptide hydrogels as collagen substitute in numerous biomedical applications. As demonstrated by the findings, changing the amino sequence resulted in distinct gelation and physico-chemical properties. In addition, the unique nanofibrous morphology of BPAA-tripeptides hydrogels, which was analogous to collagen fibers, was able to maintain the adhesion and proliferation of encapsulated L929 and MC-3T3 cells. Therefore, these peptide hydrogels showed great potential as a substitute for collagen in numerous biomedical fields.

2 Experimental section

2.1 Materials and methods

Phenylalanine, glycine, and alanine protected by Fmoc and 2-chlorotriyl chloride resin (1.01 mmol/g) were purchased by Shanghai GL biochem (China). Fetal

bovine serum (FBS, Gibco, South America origin) was provided by Life Technologies Corporation (USA). Phosphate Buffered Saline (PBS, 0.0067 M), α -Modified Eagle Medium (α -MEM) and Dulbecco's Modified Eagle Medium (DMEM) were supplied by Thermo Fisher Scientific Corporation (USA). The remaining reagents were provided by Chengdu Best-reagent Corporation (China) and applied with no additional purification. The ^1H NMR (Nuclear Magnetic Resonance) spectra were obtained on a Bruker AVII-400 (400 MHz, USA) using DMSO- d_6 as a solvent. Liquid chromatography-mass spectrometry (LC-MS) analysis was conducted on a Finnigan TSQ Quantum Ultra LC-MS system with an electrospray ionization (ESI) source.

2.2 The preparation of BPAA-tripeptides

Taking BPAA-FFG-OH as a protocol, employing 2-chlorotriyl chloride resin and phenylalanine, glycine protected by Fmoc, the synthesis process of 4-biphenylacetic acid bonding to tripeptides was carried out following uniform solid phase peptide synthesis (SPPS). To this aim, dry dichloromethane (DCM) and 2-chlorotriyl chloride resin (1.0 g) were introduced into the reaction container. Then, 2-chlorotriyl chloride resin was immersed and swelled in DCM for half an hour. Afterwards, a solution dissolving Fmoc-Gly-OH (357 mg) and *N,N*-diisopropylethylamine (DIPEA, 2.4 mmol, 420 μL) in DCM was added and mixed for 90 min. After the coupling process, the resin was bathed with DCM after the solution was cleared. Successively, the blocking solution (DCM/methanol/DIPEA = 7/2/1, v/v) was added to protect the moiety and removed after 10 min. The Fmoc-protecting group was cleared by immersing the amino acid carrying resin into DME, containing 20% piperidine (v/v) for 30 min. The subsequent Fmoc-L-Phe-OH (1.5 mmol), dissolved in DME, was added into the reaction to bond with the amino acid loaded on the resin, in presence of *O*-Benzotriazole-*N,N,N',N'*-tetramethyl-uronium-hexafluorophosphate (HBTU, 1.5 mmol) and DIPEA (3.0 mmol). Afterwards, as described above, the bonding of another Fmoc-L-Phe-OH and off-protection of the Fmoc group were repeated to lengthen the peptide chain. Subsequently, 4-biphenylacetic acid (BPAA) was connected to the peptide chain and after, BPAA (1.5 mmol), HBTU (1.5 mmol) and DIPEA (3.0 mmol), dissolved in DME, were introduced. DCM and DME were employed to purify the obtained resin, and then the product was separated from the resin by applying DCM/TFA (99:1, v/v). Finally, the resulting product was precipitated in cold diethyl ether and analyzed by mass spectrometry (MS), high performance liquid chromatography (HPLC) and ^1H NMR.

2.3 Hydrogel preparation and morphological characterization

BPAA-tripeptides solution was prepared at concentrations of 1 mM, 200 μ M, 50 μ M, 10 μ M and 2 μ M, respectively. Firstly, the compounds were dissolved in 1 mL germfree deionized water with the addition of 1 M NaOH, to adjust the solution pH value to 9, before vigorously vortex. Afterwards, 0.3 M PBS was added into the solutions, and the compound was thoroughly mixed to ensure the PBS content 0.01 M in the solution. All the solutions under treatments were required to stand for nearly half an hour with no disturbance. During the process of hydrogel formation, tube inversion assay was applied to verify the gelation time.

2.4 Rheology

The viscoelastic properties of these peptide hydrogels were analyzed with rheology measurements which were performed on a TA Discovery DHR-2 composed of an opposite circle substrate with a diameter of 40 mm and a 1.0 mm gap. A combined measurement was employed which was comprised of “amplitude sweep” and “frequency sweep”. To ensure the linear viscoelastic regime during the dynamic frequency sweep, the dynamic strain sweep was operated with a log ramp strain ranging from 0.1 to 10% and a frequency of 1 Hz.

2.5 CD and fluorescence emission measurements

An Applied Photophysics Chirscan Circular Dichroic spectrometer was employed to test the circular dichroic (CD) spectra. Considering the characteristic peak is not consistent with the concentration of sample, the concentration of peptides solution was set properly in order to obtain a relatively clear result. 2 mL gelator solution was first dropped into a quartz dish, and all the data were collected with a bandwidth of 1 nm, a step of 1 nm, a collection time of 0.5 s per point and the fluctuation of wavelengths between 190 and 350 nm.

A fluorescence spectrophotometer was employed to detect the fluorescence emission spectra. The solution of gelators or hydrogels was first dripped in a quartz dish, and all the data were collected with an excitation wavelength of 265 nm, bandwidth of 1 nm and the fluctuation of wavelengths ranging from 250 to 500 nm at 25 °C. In addition, every measurement was tested three times, and the average was plotted in the figure. Excel software was used to process all the data.

2.6 Cytotoxicity test

To estimate the cytotoxicity of gelators on L929 cells, a 3-(4,5-Dimethylthiazol-2-yl)-2,5-Diphenyltetrazolium Bromide (MTT) experiments were performed. L929 cells were cultured in DMEM with 10% FBS (v/v) and then

suspended and planted in a 96-well-plate with every single well containing 2×10^3 cells, followed by culturing for 12 h in an incubator (37 °C, 0.5% CO₂). In the meantime, the gelator solutions obtained by dissolving gelators in germfree water were diluted into a series of concentrations with culture medium. Subsequently, the gelator solution was added to the well, after cleaning the medium from the 96 well plate. The controlled group was only treated with DMEM (10% FBS). After cells incubation for 48 h, MTT solution (20 μ L, 0.5%, w/v) was introduced to every well. Then, these cell culture plates were incubated in 37 °C for 4 h. Similarly, for MC-3T3 cytotoxicity test was performed. A Thermo Scientific Varioskan Flash Multiscam Spectrum was employed to measure the absorbance at a wavelength of 490 nm, and the data were processed by Excel software.

2.7 BPAA-tripeptides hydrogels co-culture with L929 cells and MC-3T3 cells

By using trypsin (0.25%)-EDTA solution, L929 cells were trypsinized and suspended in DMEM (10% FBS). For 3-dimensional (3D) culture, BPAA-tripeptide hydrogels formed by introducing PBS in gelator solution to ensure the final ion concentration was 0.01 M. After ion induction, the gelator solutions were then blended thoroughly with a certain amount of L929 cell suspension to ensure that the cell concentration was 2×10^6 cells/mL. After the cell-hydrogel compound remained in the molds for 30 min, the gelation process was ensured. Finally, the 3D cell-encapsulated hydrogels were incubated for one week as the culture medium was changed every day.

After incubation for a certain period, live/dead assays were performed to test cells survival along with proliferation. Firstly, the hydrogel-cell compounds were gently washed with PBS to remove the excess of culture medium. Next, the compounds were washed in newly prepared live/dead dye composed of FDA and PI for 1 min until the cells were dyed. Finally, the stained compounds were placed into PBS to clear the additional FDA/PI.

After 7 days of incubation, rhodamine-phalloidin and Hoechst were applied to the cytoskeletal F-actin stain. Firstly, the excess medium in the cell-hydrogel compounds was removed with PBS. Next, 4.0% formaldehyde was dropped onto the compounds to fix the cells. Then, the compounds were submerged into rhodamine-phalloidin dye to dye the cytoskeletal F-actin completely. After 40 min, Hoechst was dropped onto the cell-hydrogel compounds and incubated for 1 min to dye the nucleus. Finally, the dyed hydrogel-cell compounds were submerged into PBS to clean out the additional dyeing solution. After dyeing, a Leica TCS SP5 confocal laser scanning microscope (CLSM) was used to observe the

fluorescent L929 cells. For MC-3T3 cells, the co-culture process with BPAA-tripeptides hydrogels was similar with L929 cells, a CLSM (LSM 880, Zeiss) was used to observe the fluorescent MC-3T3 cells.

2.8 ALP staining of BMSCs co-culture with BPAA-tripeptides

First, rabbit bone mesenchymal stem cells (rBMSCs) were cultured in α -MEM with 10% FBS (v/v) and then suspended and planted in a 24-well-plate with every single well containing 2×10^4 cells. Next, 1 mL BPAA-tripeptides solution and osteogenic induction medium were introduced into system, followed by culturing in an incubator (37 °C, 0.5% CO₂). Osteogenic induction medium and BPAA-tripeptides solution were refreshed every two days. BMSCs at the bottom of the 24-well plate were fixed after 7 days and stained by a BCIP/NBT Alkaline Phosphatase Chromogenic Kit (Beyotime, China).

2.9 Statistics

Results were presented as mean \pm standard deviations (SD). Statistical analysis was performed using one-way analysis of variance followed by Tukey's post-hoc testing using GraphPad Prism (version 8.0, GraphPad Ltd., China) software and the significance level was set at $p < 0.05$ (*), $p < 0.01$ (**), $p < 0.001$ (***)

3 Results and discussion

3.1 The design and optimization of BPAA-tripeptides

According to standard solid-phase peptide synthesis, BPAA-tripeptides were successfully synthesized using 2-chlorotrityl chloride resin and Fmoc-protected amino acids, and their structures were elucidated using proton nuclear magnetic resonance (¹H NMR) (Fig. 1). In addition, mass spectrometry (MS) and high performance liquid chromatography (HPLC) were also used to explain the chemical structures of the compounds depicted in Additional file 1: Figs. S1–S3. The MS exhibited characteristic peaks at m/z 564.19, 564.48, and 578.23, which demonstrated the successful preparation of BPAA-FFG, BPAA-GFF, and BPAA-AFF [26, 27]. The gelation properties of each BPAA-tripeptide, obtained via ion induction are shown in Table 1. Under ion induction, the BPAA-FFG-OH, BPAA-AFF-OH, and BPAA-GFF-OH peptides generated transparent and homogeneous hydrogels. Nonetheless, the remaining three peptides, BPAA-FGE, BPAA-FAE, and BPAA-FFA, precipitated during the ion induction process. As widely known, the amino acid sequence significantly influences the self-assembly of aromatic short peptide gelators [29]. Accordingly, the glycine and alanine between the biphenyl group and phenylalanine could regulate the steric hindrance in BPAA-GFF-OH and BPAA-AFF-OH, allowing the

biphenyl group to easily rotate and adjust to an appropriate location, resulting in a more efficient supramolecular arrangement. In addition, these three peptides may self-assemble into hydrogels due to the presence of sufficient π - π stacking interactions [30]. Accordingly, the two adjacent phenylalanine groups (FF) provided sufficient π - π overlapping effects for BPAA-AFF, BPAA-FFG, and BPAA-GFF to self-assemble into 3D hydrogel networks, whereas, the two non-adjacent phenylalanine could not interact so strongly, demonstrating the crucial effect of the "FF" brick on the composition of short-peptide gelators. Furthermore, these three peptides were capable of forming transparent hydrogels with a gelation concentration lower than 12 mM, indicating that the water content of the hydrogels reached 99.34 wt.%.

3.2 The self-assembled nanofibrillar structure of BPAA-tripeptides by changing the sequence of amino acid

Variations in the amino acid sequences of BPAA-tripeptides exert a dominant effect on the self-assembly properties, resulting in a distinct nanostructure [31]. Consequently, the diameter of the nanofibers was observed and measured using TEM and SEM. As depicted in Fig. 2A, the TEM images of BPAA-FFG, BPAA-GFF, and BPAA-AFF revealed long, worm-like nanofibers in the absence of ion induction. Furthermore, these worm-like nanofibers were not compacted in the tripeptides solution. However, following ion induction, all three gelators generated homogeneous and transparent hydrogels. Additionally, a rough fiber bundle was formed by the arrangement and aggregation of multiple fibers. Furthermore, all the fibers were intertwined, which accounted for the effect of ion induction. Moreover, the SEM micrographs further revealed that the nanofiber sizes in hydrogels were uniform and that these fibers were densely interwoven. Correspondingly, the nanofiber diameters of Gel-FFG, Gel-GFF, Gel-AFF, and collagen obtained from SEM images were found to be $\sim 36.60 \pm 5.16$ nm, $\sim 41.20 \pm 5.27$ nm, $\sim 36.80 \pm 3.31$ nm, and $\sim 83.20 \pm 15.83$ nm, respectively (Fig. 2D). In contrast, TEM micrographs revealed diameters of $\sim 9.40 \pm 1.50$ nm, $\sim 9.60 \pm 0.98$ nm, $\sim 4.90 \pm 0.23$ nm, and $\sim 102.40 \pm 25.73$ nm (Fig. 2E), respectively. The width of nanofibers was found to be proportional to the solution concentration. Since the concentration of samples for the TEM test was lower than that for the SEM test, therefore, the weak force between single fibers was unable to cause fibers to firmly intertwine, resulting in narrow fibers in the TEM images. In addition, as depicted in Fig. 2F, the gelation time of the hydrogels was less than 30 min. Thus, the superior properties of the nanofiber

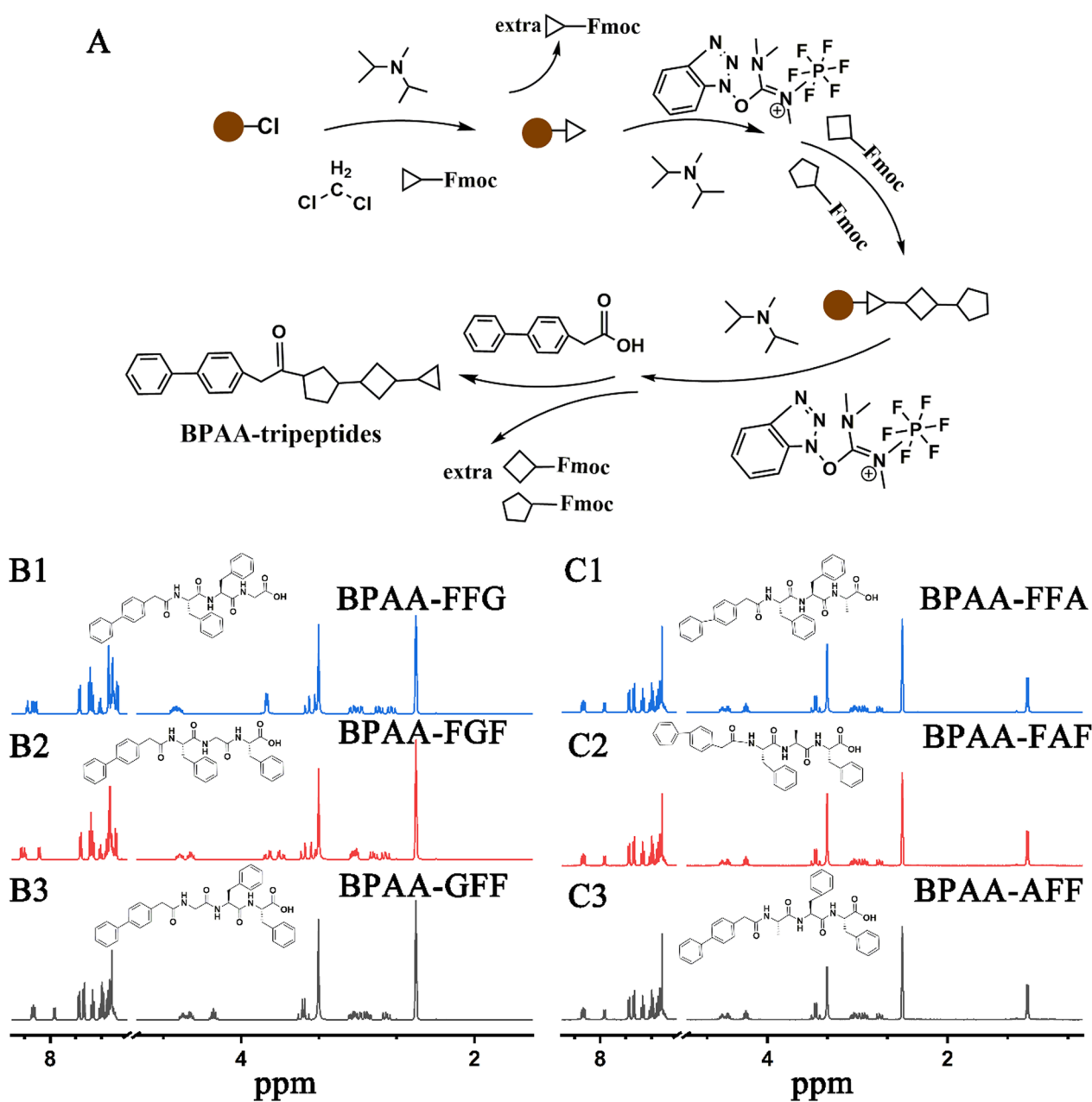


Fig. 1 A SPPS protocol of BPAA-tripeptide compounds. (B1–B3) ^1H -NMR (DMSO) spectra of BPAA-FFG-OH, BPAA-FGF-OH and BPAA-GFF-OH. (C1–C3) ^1H -NMR (DMSO) spectra of BPAA-FFA-OH, BPAA-FAF-OH and BPAA-AFF-OH

and the rapid gelation time make biomedical applications of these hydrogels possible.

3.3 Secondary structure and intermolecular interactions analyzed from CD and fluorescence emission spectroscopy

The secondary structure of the supramolecular construction was further determined using CD spectra. The CD spectra (Fig. 3A–C) demonstrated that these

three ion-induced self-assembled supramolecular hydrogels displayed a typical β -sheet structure. In particular, the two faint negative signals at approximately 197 and 220 nm ($n-\pi^*$ transition) in the CD spectra of the BPAA-FFG gel suggested that the gelators interacted via a clear β -sheet conformation [32]. In addition, the signal between 290 and 305 nm, which indicates a typical $\pi-\pi^*$ transition, confirmed the superhelical arrangement of the biphenyl groups. For the other two hydrogels, the change

Table 1 Gelation properties of BPAA tripeptide compounds

Entry	Compound	Dissolve: pH = 9	Treatment: Ion induction	MGC (mM/wt%)	Gelation time (minutes)
1	BPAA-FFG-OH	Clear solution	Transparent hydrogel	12/0.66	25.9
2	BPAA-FFA-OH	Semi-clear solution	Precipitation	n/a	n/a
3	BPAA-FGF-OH	Clear solution	Precipitation	n/a	n/a
4	BPAA-FAF-OH	Clear solution	Precipitation	n/a	n/a
5	BPAA-GFF-OH	Clear solution	Transparent hydrogel	10/0.55	26.5
6	BPAA-AFF-OH	Clear solution	Transparent hydrogel	7/0.39	26.3

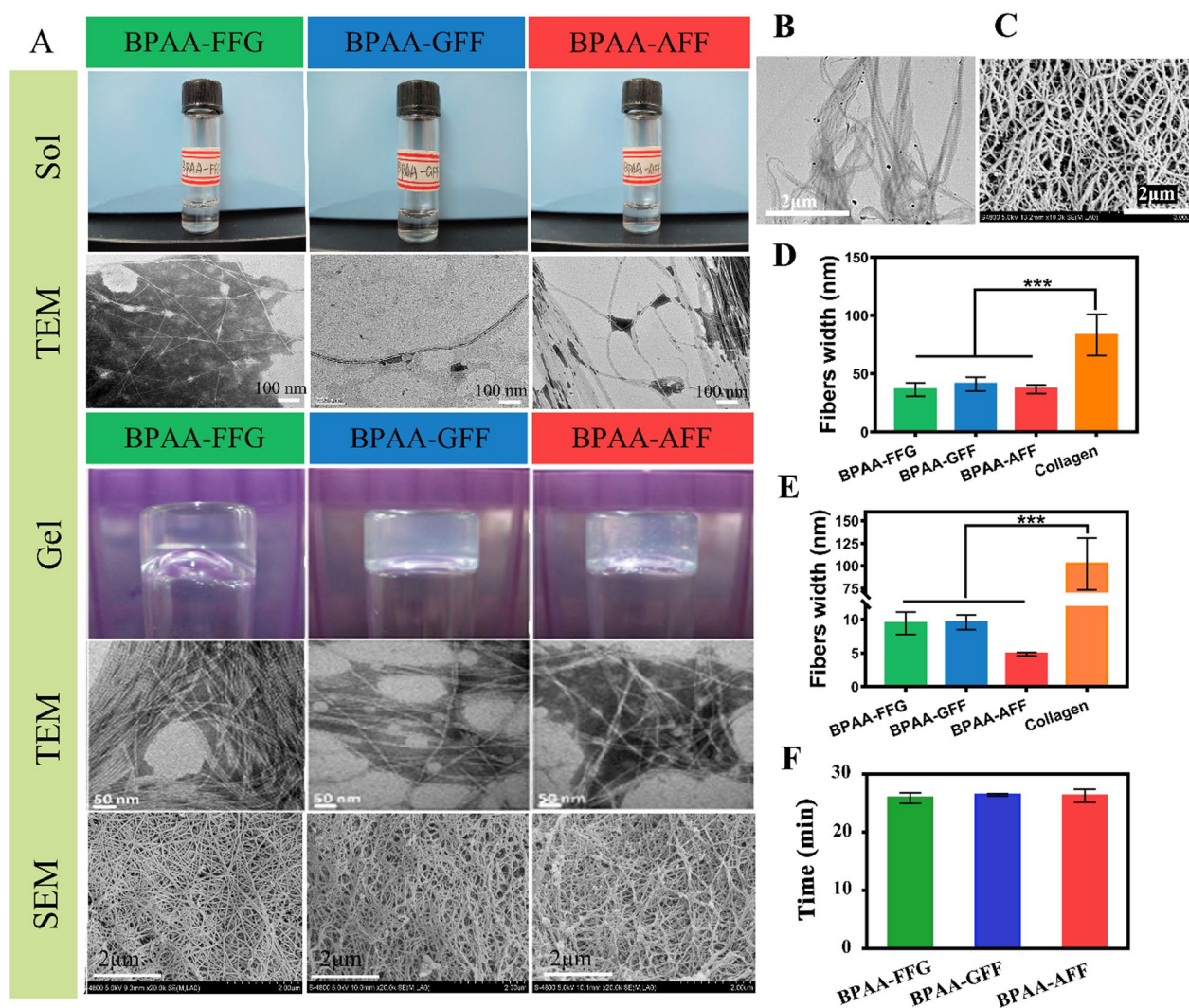


Fig. 2 **A** The optical and TEM images of BPAA-FFG, BPAA-GFF and BPAA-AFF sols along with the optical, TEM and SEM images of BPAA-FFG, BPAA-GFF and BPAA-AFF gels. **B** The TEM image of collagen. **C** The SEM image of collagen. **D** The fiber width obtained from SEM of BPAA-FFG, BPAA-GFF, BPAA-AFF and collagen. **E** The fiber width obtained from TEM images. **F** The gelation time of BPAA-FFG, BPAA-GFF and BPAA-AFF gels

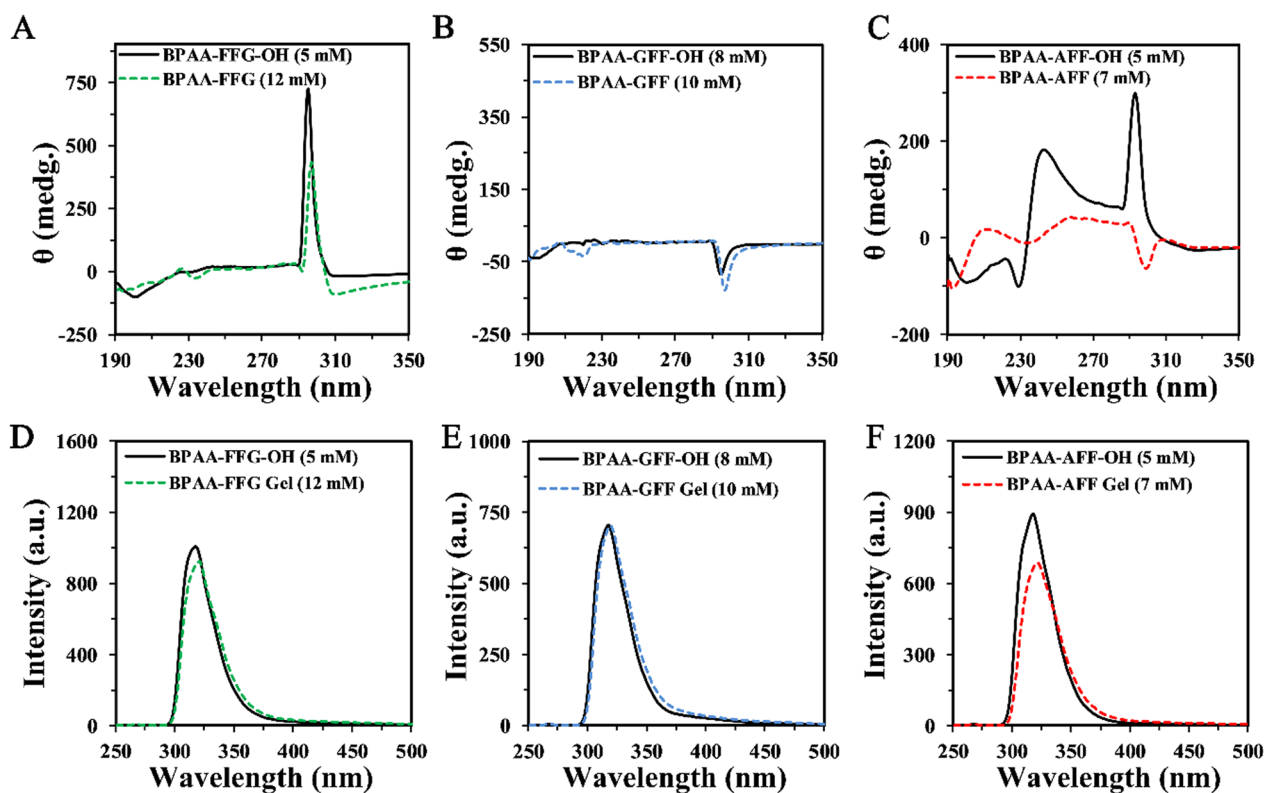


Fig. 3 A–C CD spectra of sol-FFG, sol-GFF sol-AFF and gel-FFG, gel-GFF, gel-AFF. D–F Fluorescence emission spectra of sol-FFG, sol-GFF, sol-AFF and gel-FFG, gel-GFF, gel-AFF

in signals was similar to that of BPAA-FFG analyzed from CD spectra. Following the ions' introduction, fluorescence emission spectroscopy was used to examine the interaction between the gelators (Fig. 3D–F). The fluorescence emission spectra of BPAA-FFG and BPAA-GFF solutions, respectively, exhibited intense peak signals at 317.6 and 318.2 nm. However, after introducing PBS, the emission spectra exhibited a minor redshift to 321.2 and 320.2 nm, which indicated that the biphenyl groups overlapped in an antiparallel manner [33] (Fig. 3D and E). Additionally, the fluorescence emission spectra of BPAA-AFF exhibited more pronounced redshifts from 318.2 to 324.2 nm, indicating the antiparallel conjunction of the biphenyl moiety. Correspondingly, these data demonstrated that the biphenyl groups in the nanofiber hydrogels underwent a transformation that may stabilize them, following ion induction. Accordingly, these outcomes concur well with SEM and TEM observations.

3.4 Viscoelastic property of peptides hydrogels through rheological testing

Using rheological measurements, the viscoelastic properties of the hydrogels were characterized. Accordingly,

a linear viscoelastic regime was confirmed using amplitude sweep analysis for Gel-FFG, Gel-GFF, and Gel-AFF. In addition, the strain behavior of the BPAA-GFF gel, which was characterized as a weak strain overshoot, was distinct from that of the other two hydrogels, as depicted in Fig. 4A–C. As the amplitude increased, the viscous modulus (G'') also increased, and then decreased insignificantly. Conversely, the elastic modulus (G') decreased when the amplitude value exceeded 1%. Accordingly, the amplitude was set to 0.5% for the frequency sweep analysis, which was within the linear viscoelastic regime. The oscillating rheometrical data confirmed the formation of hydrogel because the value of G'' was less than G' (Fig. 4D–F). Moreover, when the amplitude was set to 0.5%, the Gel-GFF and Gel-AFF produced by ion induction were found to be less dependent on frequency. Accordingly, the elastic moduli of Gel-GFF and Gel-AFF were ~ 0.27 and ~ 0.25 kPa, respectively. In addition, Gel-FFG, whose G' rose with the increasing frequency, exhibited a higher frequency dependence than the other two hydrogels. This may be ascribed to the structure of BPAA-FFG. Moreover, the steric hindrance between the "FF" brick and the biphenyl group hindered the

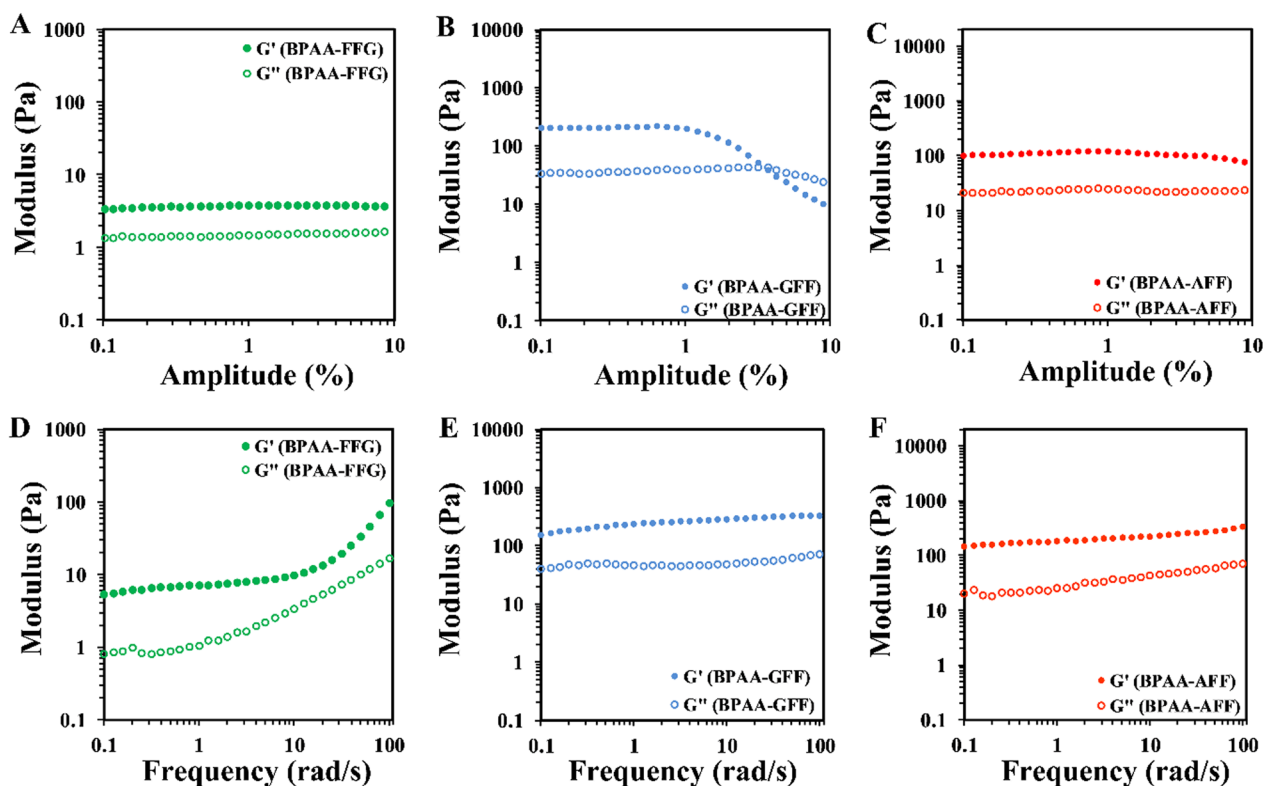


Fig. 4 A–C Amplitude sweep analysis of BPAA-FFG, BPAA-GFF and BPAA-AFF hydrogels (Frequency = 1 Hz). D–F Frequency sweep analysis of BPAA-FFG, BPAA-GFF and BPAA-AFF hydrogels (Strain = 0.5%)

movement of the molecular chain, when it was subjected to high-frequency stress.

3.5 Impact of amino acid sequence change on biological properties

To investigate the biocompatibility of BPAA-tripeptides, L929 cells were co-cultured with the peptide gelators for 7 days. Subsequently, MTT assay was performed to assess cell viability and survival. After 7 days of culture, the L929 cell profile changed from round to spindle, indicating that the cells adhered and spread across the hydrogels (Fig. 5A). MC-3T3 cells were also employed to further clarify the effects on cells. The CLSM images suggested that MC-3T3 cells in three hydrogels spread well and maintained their morphology (Fig. 5B and C). Thus, the cell survival and viability tests revealed that the BPAA-FFG and BPAA-AFF hydrogels were biocompatible and non-toxic at a concentration of 1 mM, suggesting the collagen-like structure of BPAA-FFG and BPAA-AFF was beneficial for L929 and MC-3T3 growth (Fig. 5D, E and Additional file 1: Fig. S4). However, L929 survival rate decreased with the increase of BPAA-GFF, and no significant difference among these groups was observed.

Additionally, cytoskeletal F-actin staining was carried out to detect L929 cell adhesion and spread on the hydrogels after one week. CLSM images revealed that the nuclei of the cells (blue) were surrounded by highly extended actin filaments (red), indicating the obvious adhesive growth of L929 cells (Fig. 6A). Moreover, SEM analysis showed that L929 cells adhered to the hydrogels with their characteristic morphology, which suggested the BPAA-tripeptides fibers provided adhesion sites for L929 cells (Fig. 6A). Figure 6B–D provided additional quantitative analysis of L929 proliferation and survival from MTT assay. As evident from the images, when the culture period was extended from 1 to 7 days, the absorbance at 490 nm of the three peptide hydrogels increased, indicating that L929 cells could proliferate normally in these substances.

Furthermore, to fully explain the effect of BPAA-tripeptides on cell differentiation, ALP staining was applied on BMSCs by co-culture with three BPAA-tripeptides solutions for 7 days. As shown in Fig. 6E, the ALP secretion level indicated there was no significant difference between BPAA-tripeptides and blank group. The semi-quantitative analysis also showed the same

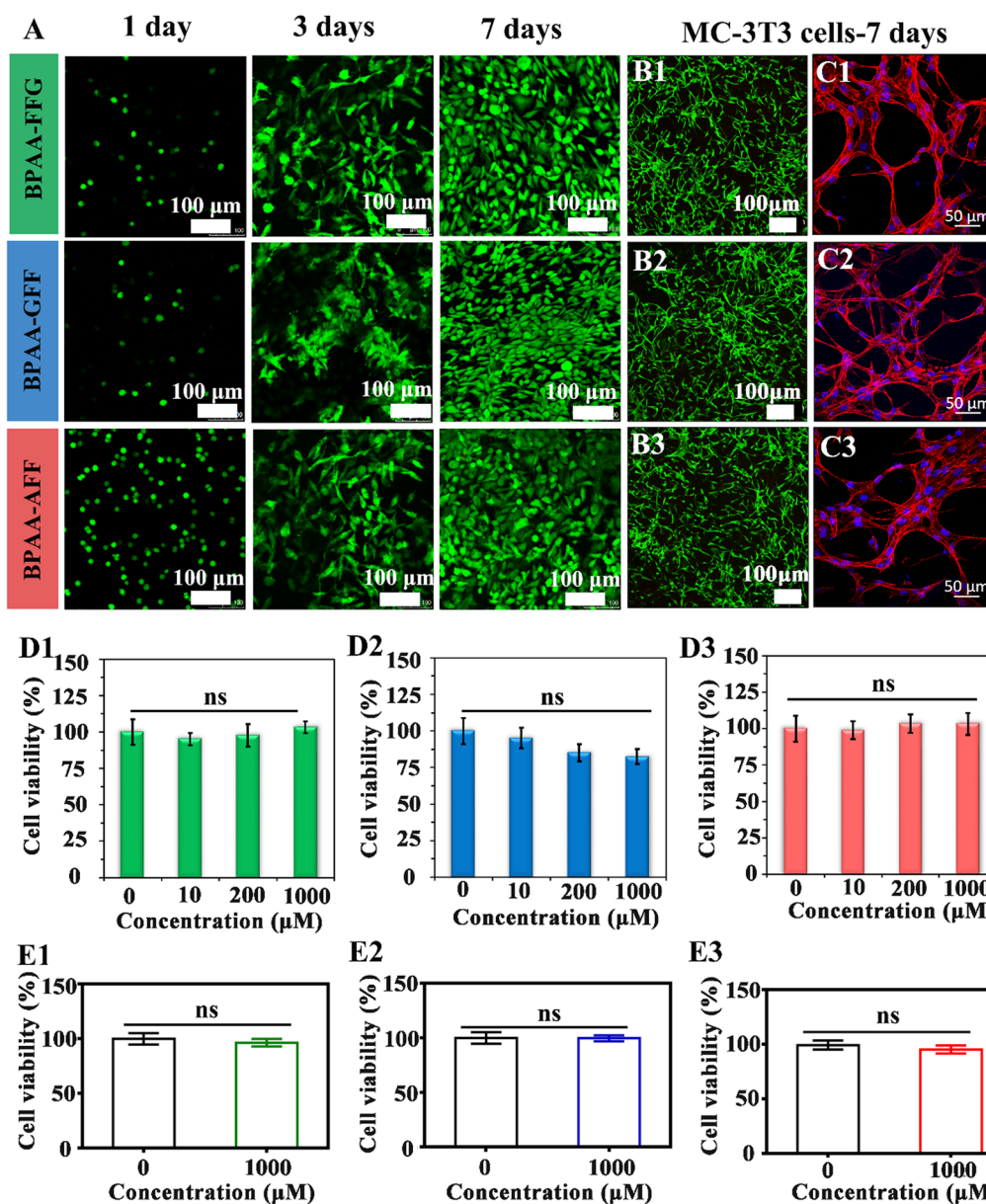


Fig. 5 **A** CLSM images (FDA/PI staining) of L929 cells encapsulated into Gel-FFG, Gel-GFF and Gel-AFF. **B1–B3** CLSM images (FDA/PI staining) of MC-3T3 cells encapsulated into Gel-FFG, Gel-GFF and Gel-AFF. **C1–C3** CLSM images (Rhodamine-phalloidin/DAPI staining) of MC-3T3 cells encapsulated into Gel-FFG, Gel-GFF and Gel-AFF. **D1–D3** The viability of L929 cells encapsulated into the hydrogels with different concentration of BPAA-FFG, BPAA-GFF and BPAA-AFF. **E1–E3** The viability of MC-3T3 cells encapsulated into the hydrogels with different concentration of BPAA-FFG, BPAA-GFF and BPAA-AFF

effect, suggesting the BPAA-tripeptides could not interfere into BMSCs differentiation process (Fig. 6F). These findings demonstrated that collagen-like supramolecular hydrogels had the ability to maintain normal cellular activities, implying their potential application prospect as cell carriers.

4 Conclusion

Here, we prepared and characterized a series of collagen-like fibrous hydrogels generated from BPAA-peptides with transposition of the primary amino acid sequence. The materials were fully characterized in terms of physico-chemical, morphological and biological behavior.

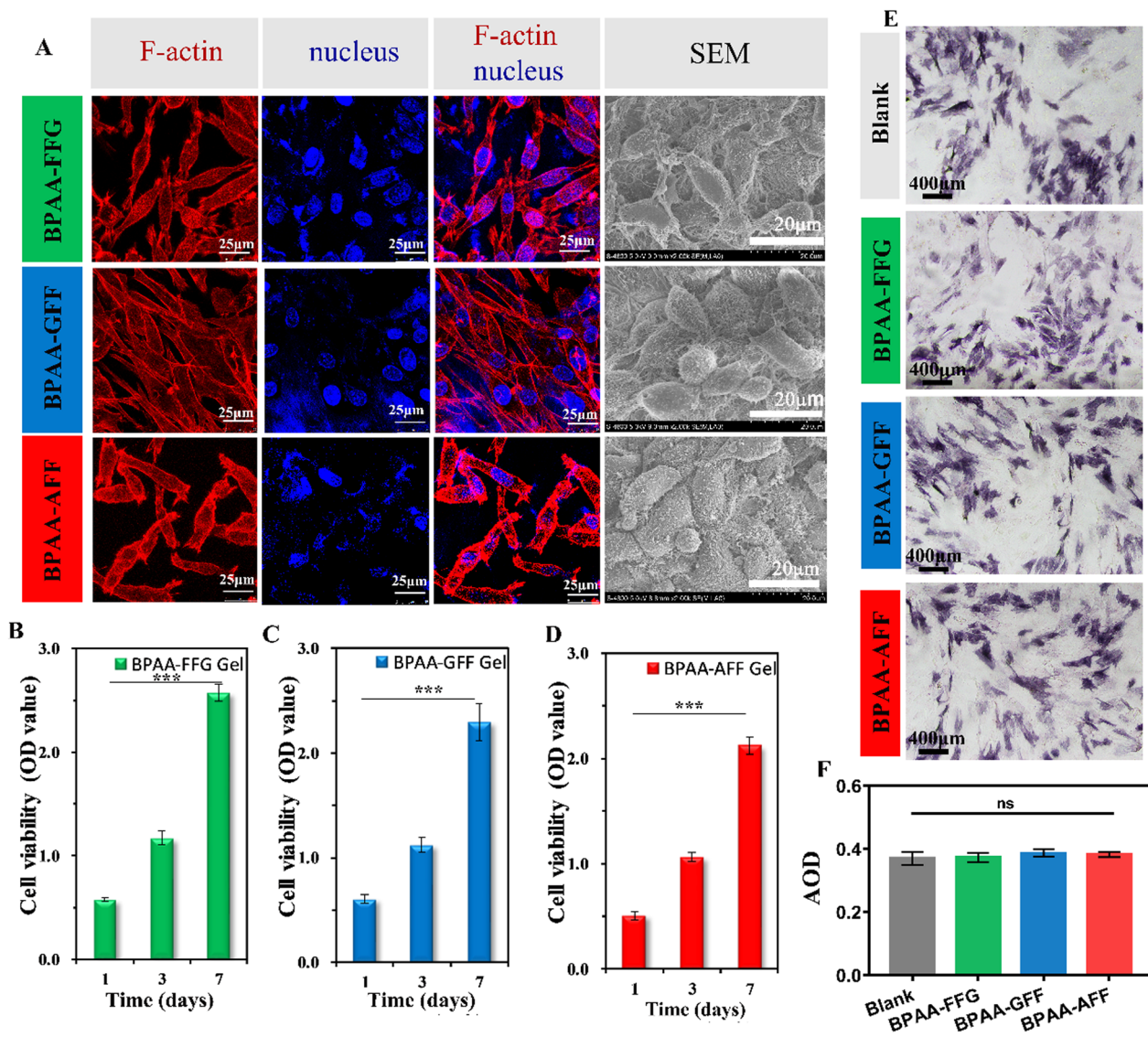


Fig. 6 **A** CLSM images (Rhodamine-phalloidin/Hoechst staining) and SEM images of L929 cells encapsulated into Gel-FFG, Gel-GFF and Gel-AFF. **B–D** The proliferation of L929 cells encapsulated into Gel-FFG, Gel-GFF and Gel-AFF during 7 days incubation. **E, F** ALP staining images of BMSCs cultured in MEM and BPAA-tripeptides, and semiquantitative analysis by image J software

The physico-chemical properties, such as nanostructure morphology and nanofiber width, resulted from distinct amino acid sequences. The minimum gelation concentration (MGC) via ion induction was less than 12 mM or 0.66 wt%, which corresponded to a water content of approximately 99.34 wt%, and the maximum elastic modulus was about 0.27 kPa. In addition, the structures of BPAA-tripeptides were similar to collagen, which was

considered an extracellular substitute, as revealed by the SEM images. The self-assembly was facilitated by the unique “FF” brick and the overlap of biphenyl groups. Finally, the supramolecular peptide hydrogels completely sustained L929 and MC-3T3 cell spreading and proliferation as a 3D scaffold. Therefore, these results suggested that BPAA-tripeptide hydrogels have a great potential as cell carriers.

Supplementary Information

The online version contains supplementary material available at <https://doi.org/10.1186/s42825-022-00110-6>.

Additional file 1: Fig. S1. The MS and HPLC spectra for BPAA-FFG. **Fig. S2.** The MS and HPLC spectra for BPAA-GFF. **Fig. S3.** The MS and HPLC spectra for BPAA-AFF. **Fig. S4. A** The viability of L929 cells co-cultured with BPAA-FFG, BPAA-GFF and BPAA-AFF solutions with a concentration of 2 μM and 50 μM

Acknowledgements

This work was sponsored by National Nature Science Foundation of China (32071352 and 81860392), Sichuan provincial Key R&D Program of China (2020YFS0462) and National Key R&D Project of China (2018YFC1105900).

Author contributions

CZ drafted the manuscript. XL and SB conducted the sample preparation and characterization. WZ and QJ supervised the project, conceived the original idea, designed the figures, revised the manuscript and proof outline. UD, AR, MR and LA revised the manuscript. JL, YS, YF and XZ provided the project administration. All the authors discussed the results and finalized the manuscript.

Funding

Not applicable.

Availability of data and materials

All data generated or analyzed during this study are included in this published article.

Declarations

Ethics approval and consent to participate

Not applicable.

Consent for publication

Not applicable.

Competing interests

The authors declare that they have no competing interests.

Author details

¹National Engineering Research Center for Biomaterials, Sichuan University, 29# Wangjiang Road, Chengdu 610064, People's Republic of China.

²College of Biomedical Engineering, Sichuan University, 29# Wangjiang Road, Chengdu 610064, People's Republic of China. ³Shenzhen Institutes of Advanced Technology, Chinese Academy of Sciences, Shenzhen 518055, People's Republic of China. ⁴Orthopedic Research Institution, Department of Orthopedics, West China Hospital, Sichuan University, Chengdu 610041, People's Republic of China. ⁵Institute of Polymers, Composites and Biomaterials, National Research Council, 80125 Naples, Italy.

Received: 8 November 2022 Revised: 22 December 2022 Accepted: 28 December 2022

Published online: 14 January 2023

References

- Avila Rodriguez MI, Rodriguez Barroso LG, Sanchez ML. Collagen: a review on its sources and potential cosmetic applications. *J Cosmet Dermatol*. 2018;17(1):20–6.
- Zhu JY, Li ZL, Zou YP, Lu GG, Ronca A, D'Amora U, Liang J, Fan YJ, Zhang XD, Sun Y. Advanced application of collagen-based biomaterials in tissue repair and restoration. *J Leather Sci Eng*. 2022;4(1):30.
- Li ZL, Cao HF, Xu Y, Li X, Han XW, Fan YJ, Jiang Q, Sun Y, Zhang XD. Bioinspired polysaccharide hybrid hydrogel promoted recruitment and chondrogenic differentiation of bone marrow mesenchymal stem cells. *Carbohydr Polym*. 2021;267: 118224.
- Chang SW, Shefelbine SJ, Buehler MJ. Structural and mechanical differences between collagen homo- and heterotrimers: relevance for the molecular origin of brittle bone disease. *Biophys J*. 2012;102:640–8.
- Rico-Llanos GA, Borrego-González S, Moncayo-Donoso M, Becerra J, Visser R. Collagen type I biomaterials as scaffolds for bone tissue engineering. *Polymers*. 2021;13(4):599.
- Sun A, He XY, Ji X, Hu DR, Qian ZY. Current research progress of photopolymerized hydrogels in tissue engineering. *Chin Chem Lett*. 2021;32(7):2117–26.
- Liao JF, Han RX, Wu YZ, Qian ZY. Review of a new bone tumor therapy strategy based on bifunctional biomaterials. *Bone Res*. 2021;9(1):18.
- Ou QM, Zhang SH, Fu CQ, Yu L, Xin PK, Gu ZP, Cao ZY, Wu J, Wang Y. More natural more better: triple natural anti-oxidant puerarin/ferulic acid/poly-dopamine incorporated hydrogel for wound healing. *J Nanobiotechnol*. 2021;19(1):237.
- Bai Y, An N, Chen D, Liu YZ, Liu CP, Yao H, Wang C, Song X, Tian W. Facile construction of shape-regulated beta-cyclodextrin-based supramolecular self-assemblies for drug delivery. *Carbohydr Polym*. 2020;231: 115714.
- Aida T, Meijer EW, Stupp SI. Functional supramolecular polymers. *Science*. 2012;335:813–7.
- Tomasini C, Castellucci N. Peptides and peptidomimetics that behave as low molecular weight gelators. *Chem Soc Rev*. 2013;42:156–72.
- Jayawarna V, Ali M, Jowitt TA, Miller AF, Saiani A, Gough JE, Ulijn RV. Nanostructured hydrogels for three-dimensional cell culture through self-assembly of fluorenylmethoxycarbonyl-dipeptides. *Adv Mater*. 2006;18:611–4.
- Frederix PW, Scott GG, Abul-Hajja YM, Kalafatovic D, Pappas CG, Javid N, Hunt NT, Ulijn RV, Tuttle T. Exploring the sequence space for (tri-) peptide self-assembly to design and discover new hydrogels. *Nat Chem*. 2015;7:30–7.
- Li XL, Liu H, Yu AL, Lin D, Bao ZS, Wang YQ, Li XY. Bioinspired self-assembly supramolecular hydrogel for ocular drug delivery. *Chin Chem Lett*. 2021;32:3936–9.
- Wang LL, Chen L, Wang JP, Wang LY, Gao CY, Li B, Wang YZ, Wu J, Quan CY. Bioactive gelatin cryogels with BMP-2 biomimetic peptide and VEGF: a potential scaffold for synergistically induced osteogenesis. *Chin Chem Lett*. 2022;33(4):1956–62.
- Yuan Y, Nie TQ, Fang YF, You XR, Huang H, Wu J. Stimuli-responsive cyclodextrin-based supramolecular assemblies as drug carriers. *J Mater Chem B*. 2022;10(13):2077–96.
- Kuang Y, Shi JF, Li J, Yuan D, Alberti KA, Xu QB, Xu B. Pericellular hydrogel/nanonets inhibit cancer cells. *Angew Chem Int Ed Engl*. 2014;53:8104–7.
- Cai YB, Zhan J, Shen HS, Mao D, Ji SL, Liu RH, Yang B, Kong DL, Wang L, Yang ZM. Optimized ratiometric fluorescent probes by peptide self-assembly. *Anal Chem*. 2016;88:740–5.
- Álvarez Z, Kolberg-Edelbrock AN, Sasselli IR, Ortega JA, Qiu R, Syrgiannis Z, Mirau PA, Chen F, Chin SM, Weigand S, Kiskinis E, Stupp SI. Bioactive scaffolds with enhanced supramolecular motion promote recovery from spinal cord injury. *Science*. 2021;374:848–56.
- Wang YH, Li XX, Zheng DB, Chen YM, Zhang ZH, Yang ZM. Selective degradation of PD-L1 in cancer cells by enzyme-instructed self-assembly. *Adv Funct Mater*. 2021;31:2102505.
- Wang HM, Feng ZQ, Del Signore SJ, Rodal AA, Xu B. Active probes for imaging membrane dynamics of live cells with high spatial and temporal resolution over extended time scales and areas. *J Am Chem Soc*. 2018;140:3505–9.
- Fleming S, Ulijn RV. Design of nanostructures based on aromatic peptide amphiphiles. *Chem Soc Rev*. 2014;43:8150–77.
- Poater J, Sola M, Bickelhaupt FM. Hydrogen-hydrogen bonding in planar biphenyl, predicted by atoms-in-molecules theory, does not exist. *Chemistry*. 2006;12:2889–95.
- Yang XY, Zhang GX, Zhang DQ. Stimuli responsive gels based on low molecular weight gelators. *J Mater Chem*. 2012;22:38–50.
- Bian SQ, Cai HX, Cui YN, He MM, Cao WX, Chen XN, Sun Y, Liang J, Fan YJ, Zhang XD. Temperature and ion dual responsive biphenyl-dipeptide supramolecular hydrogels as extracellular matrix mimic-scaffolds for cell culture applications. *J Mater Chem B*. 2017;5:3667–74.

26. Li X, Bian SQ, Zhao MD, Han XW, Liang J, Wang KF, Jiang Q, Sun Y, Fan YJ, Zhang XD. Stimuli-responsive biphenyl-tripeptide supramolecular hydrogels as biomimetic extracellular matrix scaffolds for cartilage tissue engineering. *Acta Biomater.* 2021;131:128–37.
27. Sun Y, Li X, Zhao MD, Chen YF, Xu Y, Wang KF, Bian SQ, Jiang Q, Fan YJ, Zhang XD. Bioinspired supramolecular nanofiber hydrogel through self-assembly of biphenyl-tripeptide for tissue engineering. *Bioact Mater.* 2022;8:396–408.
28. Reches M, Gazit E. Casting metal nanowires within discrete self-assembled peptide nanotubes. *Science.* 2003;300(5619):625–7.
29. Jeong B, Bae YH, Kim SW. Thermoreversible gelation of PEG–PLGA–PEG triblock copolymer aqueous solutions. *Macromolecules.* 1999;32:7064–9.
30. Adams DJ, Mullen LM, Berta M, Chen L, Frith WJ. Relationship between molecular structure, gelation behaviour and gel properties of Fmoc-dipeptides. *Soft Matter.* 2010;6:1971–80.
31. Li XM, Gao Y, Kuang Y, Xu B. Enzymatic formation of a photoresponsive supramolecular hydrogel. *Chem Commun (Camb).* 2010;46:5364–6.
32. Castilla AM, Wallace M, Mears LL, Draper ER, Douth J, Rogers S, Adams DJ. On the syneresis of an OPV functionalised dipeptide hydrogel. *Soft Matter.* 2016;12:7848–54.
33. Yang ZM, Gu HW, Zhang Y, Wang L, Xu B. Small molecule hydrogels based on a class of antiinflammatory agents. *Chem Commun.* 2004;2:208–9.

Publisher's Note

Springer Nature remains neutral with regard to jurisdictional claims in published maps and institutional affiliations.

Submit your manuscript to a SpringerOpen[®] journal and benefit from:

- Convenient online submission
- Rigorous peer review
- Open access: articles freely available online
- High visibility within the field
- Retaining the copyright to your article

Submit your next manuscript at ► [springeropen.com](https://www.springeropen.com)
